

Search for the prewave zone effect in transition radiation

M. Castellano and V. Verzilov*
INFN-LNF, P.O. Box 13, I-00044 Frascati, Italy

L. Catani and A. Cianchi
INFN-Roma 2, 00100 Roma, Italy

G. D'Auria, M. Ferianis, and C. Rossi†
Sincrotrone Trieste, S.S. 14 Km. 163.5, 34012 Trieste, Italy
 (Received 11 October 2002; published 9 January 2003)

Results of the first experimental search for the effect of the prewave zone in near-infrared transition radiation are presented. A substantial difference in the spatial distribution of transition radiation for two different wavelengths (450 nm and 1600 nm) was observed. Experimental data are in a good, though not complete, agreement with the theory.

DOI: 10.1103/PhysRevE.67.015501

PACS number(s): 41.60.-m, 41.75.Ht

Though transition radiation (TR) has been a subject of extensive theoretical and experimental investigations for nearly 50 y, some recent studies indicate that, probably, our knowledge of this phenomenon is still not complete. It was shown recently [1,2] that the effect of the finite size of the target, used to generate TR, may strongly affect radiation angular and spectral characteristics when the parameter $\lambda\gamma$ (here λ is a wavelength and γ is the relativistic factor), which is a measure of the transverse extension of the Coulomb field of a relativistic charged particle at a given harmonic, exceeds the target dimensions. The experimental evidence of this effect was reported in Ref. [3].

Considering spatial distributions of TR at close and far distances from the target, it was pointed out [4,5] that at distances R , such that $R \leq \lambda\gamma^2$, the radiation evolves in a different way from what one could expect relying on the conventional far-field theory. The intuitive explanation is that, while at long distances (known as the far-field or wave zone) the radiation source can be considered a pointlike and the radiation field can be written in its asymptotic form of an outgoing spherical wave, at closer distances, i.e., in the prewave zone, this is no longer true. In the prewave zone the radiation behaves as being emitted by an extended source and thus the asymptotic form is no longer valid. As a result, the radiation characteristics vary significantly with the frequency and distance from the source gradually acquiring their far-field form at $R \gg \lambda\gamma^2$. It should be noted that basically the same condition for applicability of the far-field approximation was derived earlier for the case of diffraction [6] and edge [7] radiations.

This paper presents results of the experimental search for the effect of the prewave zone in transition radiation. The simplest strategy, consisting in measuring the spatial distribution

of the TR radiant energy at two well-separated wavelengths, was chosen for this experiment. According to the conventional theory no wavelength depending effects should be present, while Ref. [4] predicts such kind of effects in the prewave zone.

Planning the experiment, the key point was, in our opinion, to keep experimental conditions unchanged during the whole measurements and to make use of the same detector for both wavelengths. Preliminary estimates, taking into account the available beam energy and quality, have shown that the spectral range of interest spanned the visible and near-infrared regions. At this point, the choice of the detector was not trivial. A standard CCD camera is operational in the visible range where the effect is small. Furthermore, it appeared to be not sensitive enough for our beam intensity. Existing infrared cameras, as a rule, operate solely in the infrared domain. Eventually, a photomultiplier tube (PMT) was preferred, but at the expense of seriously complicating the experiment. With a PMT the spatial distribution can be measured by placing a small pinhole in front of the photocathode and performing transverse scans by moving the whole system across the radiation cone in steps. If the pinhole is sufficiently small, a single scan gives a profile of the intensity distribution.

A Hamamatsu R5509-72 PMT was chosen as it has a rather flat quantum efficiency (0.5–2%) in the 300–1700 nm wavelength range of interest. The photocathode active area is $3 \times 8 \text{ mm}^2$. The measured uniformity of the sensitivity across the cathode surface was better than 20%. To provide a high sensitivity by keeping the thermal noise at low levels, the PMT was operated at -80°C by continuous cooling with liquid nitrogen.

The experiment was performed at the 1 GeV Linac, presently used as the injector for the ELETTRA storage ring, whose main parameters are given in Table I.

The geometry of the experiment was determined by the beam energy and the longer wavelength. As a practical limit to the distance z from the source for which the prewave zone effects are observable, the following condition was used:

*Present address: Sincrotrone Trieste, S.S. 14 Km. 163.5, 34012 Trieste, Italy.

†Present address: CERN, 1211, Geneva 23, Switzerland.

TABLE I. Linac main parameters.

Beam energy	0.9 GeV
Beam current	10 mA
Pulse duration	70 ns
Repetition rate	10 Hz
Energy spread	0.5%
Normalized emittance	150π mm mrad

$$z \leq \frac{\lambda \gamma^2}{2\pi}. \quad (1)$$

For a given wavelength, the relative effect is larger the closer the detector is to the target. However, the spatial resolution of the system is a limiting factor at close distances. In fact, the central part of the TR intensity distribution, most valuable from the point of view of the experiment, scales like z/γ and must, therefore, be measured at distances sufficient to provide the necessary resolution. Apart from resolution, the beam size and its angular divergence may strongly distort the measurements at close distances.

As a reasonable compromise, the distance between the target and the detector was chosen to be 80/100 cm. At such a distance, Ref. [4] predicts a difference of a factor of 2 in the position of the maxima with respect to the center in profile measurements, when going to the longest wavelength. However, as it appeared later, it was not possible to perform the profile measurements, nor take full advantage of the high sensitivity of the PMT. The reason was the background due to unavoidable beam losses, which are synchronous with the beam. The whole dynode system is extremely sensitive to the high-energy background and this considerably lowered the signal-to-noise ratio. Since the PMT was located close to the beam line, even a heavy lead shielding could not completely solve the problem. After a series of trials, we found that the only solution was to use a slit instead of a pinhole. An optimal compromise between spatial resolution and signal-to-noise ratio was found with a vertical slit size of 300 μm . In the horizontal direction, the resolution was limited by the cathode size, i.e., 3 mm. The price we paid for replacing a pinhole with a rectangular slit was a significantly reduced observable effect that pushed us to work on the extreme wavelengths of the range of the PMT sensitivity.

The experimental setup is schematically shown in Fig. 1. TR was generated by the electron beam on the mirror-quality surface of a target placed at 45 deg with respect to the beam, so that radiation came out of the vacuum chamber orthogonal to the beam axis. A set of two interference filters with a 450 nm and 1600 nm central wavelength and bandwidth of 40 nm and 90 nm, respectively, were mounted on a rotating wheel and used to select a narrow band of the incoming light spectrum. The target was a 0.3-mm thick aluminum coated silicon plate with transverse dimensions of 40×50 mm. The effect of the target dimensions on radiation characteristics is negligible even at the wavelength of 1600 nm. The filtered light then passed through the horizontal 300- μm wide slit

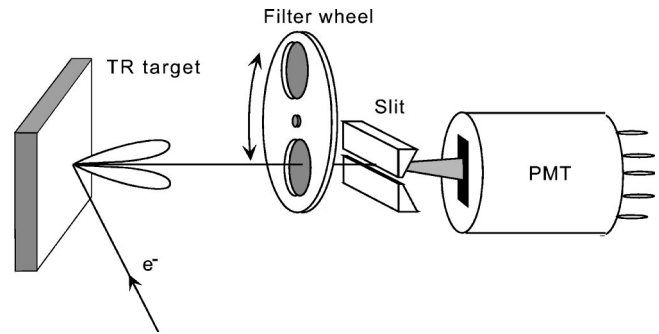


FIG. 1. Schematic layout of the experiment. TR generated by the beam was filtered by either of the two narrow-band filters, passed through a horizontal slit, and collected on the photocathode of a PMT. Filters, slit, and PMT are all mounted on a common remotely movable support.

and impinged on the photocathode. The distance between the target and the slit was 80 cm, that between the slit and the photocathode was 14 cm. Filter wheel, slit, and PMT were mounted on the same support, which could be moved in all three dimensions by means of stepping motors. The position was measured by a simple, potentiometer based, readout system with a resolution of 25 μm .

One of our major concerns was diffraction on the slit aperture generating a fringe pattern on the photocathode surface. However, calculations showed that in the worst case of the 1600 nm wavelength the total width of the diffraction pattern on the photocathode including up to third-order maxima is only 4 mm, which is considerably smaller than the photocathode vertical size of 8 mm. Due to the change in the incident angle during a scan, the diffraction pattern moves on the cathode by a value $\Delta = y/l/L$, where y is a slit position with respect to the radiation axis (the central minimum), l and L are slit-to-cathode and target-to-slit distances. In our case the maximum excursion is less than 2 mm over the whole range of a typical scan, so we estimate the effect of diffraction as negligible.

Figure 2 shows two scans measured at the wavelengths of 450 and 1600 nm in 100 μm steps. The vertical errors on the experimental points are statistical, while the horizontal ones are due to the position readout signal uncertainty. Solid lines are theoretical calculations based on formulas given in Ref. [5]. Concerning calculations the following details should be mentioned.

Results of Ref. [5] were obtained for the case of normal incidence, but given the high beam energy and the mirror polish of the target surface, they are directly applicable to our 45° incidence case too.

Measurements in the prewave zone are affected not only by the beam size and angular divergence, but by their possible correlation as well. To deal with these effects in a rigorous way, detailed information about the beam phase space distribution would be necessary. Since, this kind of information was not available, we described the overall effect by convoluting single-particle distributions of Ref. [5] with a Gaussian and varied its dispersion parameter to obtain a reasonable agreement between the theory and the experiment in

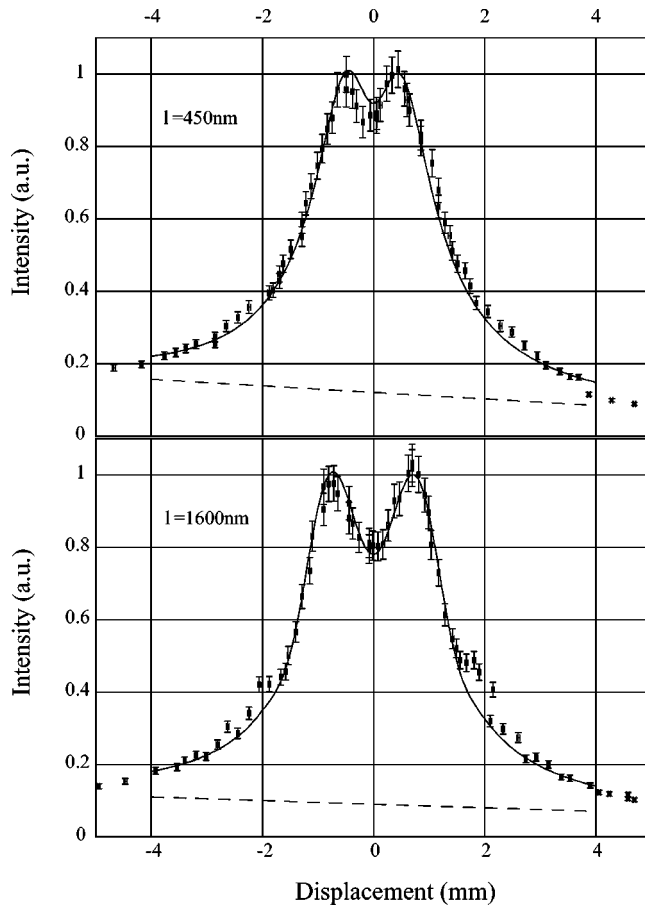


FIG. 2. Normalized radiation intensity versus vertical displacement of the measuring system (scan), for two different wavelengths. The scan step is $100 \mu\text{m}$. Solid lines are theoretical calculations and dashed ones indicate fit of background level.

the central minimum. Obviously, the same value of the parameter was used for both wavelengths.

All experimental curves are normalized to their maxima. A small background contribution was added to the theoretical distributions to agree with the experiment at tails.

To improve spatial resolution of the experiment, in addition to wide-range scans, we also performed measurements of the central part of the intensity distribution reducing the scan step down to $50 \mu\text{m}$. Data obtained in this way are present in Fig. 3. The background and normalizing coefficient were taken to be the same as in the corresponding complete scan.

Experimental data in Figs. 2 and 3 for different wavelengths can be compared to each other and with theory in terms of the shape of distributions, position of the peaks and central minimum depth intensity. As seen from both figures, the agreement between experiment and the theory is very good, except for some structure in the tails of the distribution, not present in the theoretical curves. The comparison between the two wavelengths shows that the distance between the peaks vary by almost 50%. As a consequence, the depth of the central minimum differs by 10%.

In the second run, the experiment was slightly modified in

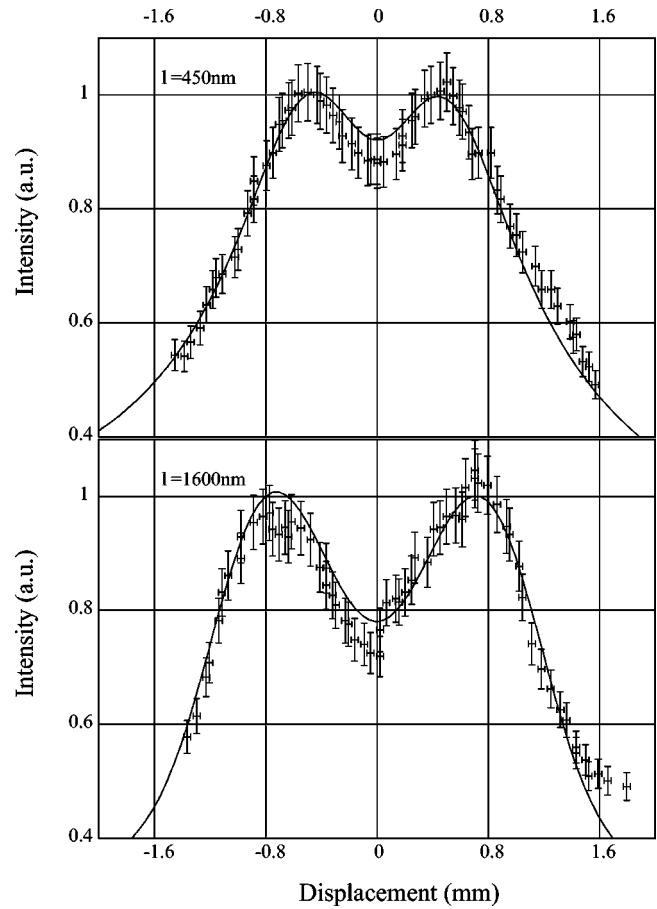


FIG. 3. $50 \mu\text{m}$ step scans of the central part of the intensity distribution. Background levels and normalization coefficients are the same as in the full-range scan (Fig. 2).

order to measure only the vertical polarization component of the radiation. To this end we made use of a Glan-Taylor polarizing prism with a $350\text{--}2300 \text{ nm}$ operational wavelength range. The prism with a diameter of 10 mm and a length of 17.5 mm was placed in front of the slit. Results of the measurement and theoretical curves for this case are shown in Figs. 4 and 5. The agreement between theory and experiment is not so good as for the nonpolarized case. In particular, for the 1600 nm wavelength, the experimental curve is narrower than the theory predicts. Nevertheless, the difference of about 20% in the interpeak distance and of 50% in the central minimum depth is clearly observed.

One feature common to most of the scans should be noted, namely, the presence of a structure in the tails of distributions, especially evident in the case of the 1600 nm wavelength (Figs. 2 and 4). In spite of a thorough analysis of the experimental situation, we could not decide whether this structure comes from the background or is a property of the radiation.

In conclusion, we note that an experimental search for the effect of the prewave zone in TR was undertaken. We measured the spatial distribution of TR at two distantly separated wavelengths and observed a difference between the two cases in good agreement with the theory. More detailed ex-

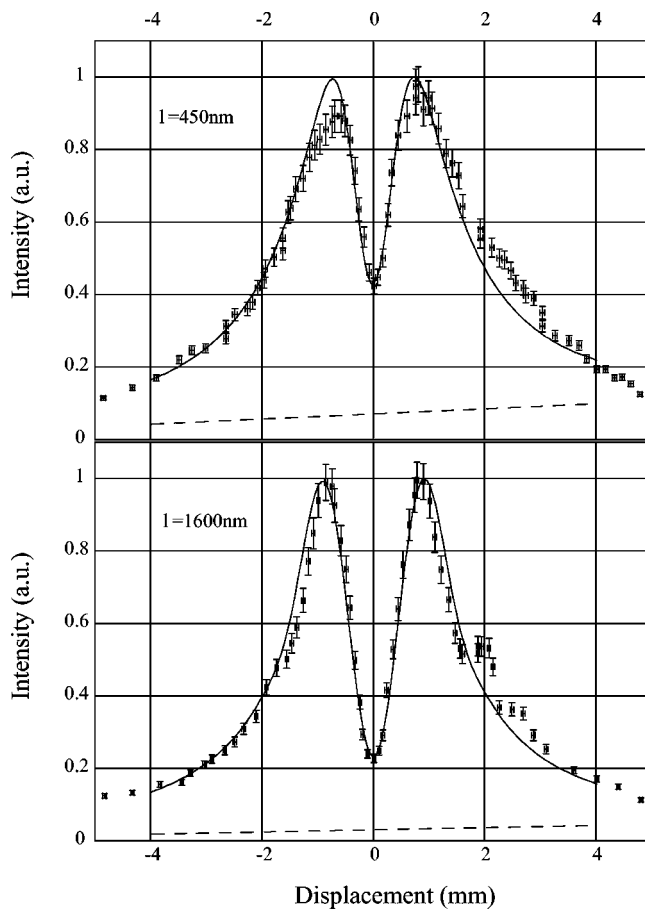


FIG. 4. Full-range scans of the vertically polarized component of radiation. Step is $100 \mu\text{m}$. Solid lines are theoretical calculations and dashed ones indicate assumed background levels.

perimental studies are needed under different experimental conditions, preferably with higher beam energy and intensity, since then all the measurements could be performed in the visible using a simple CCD-like device.

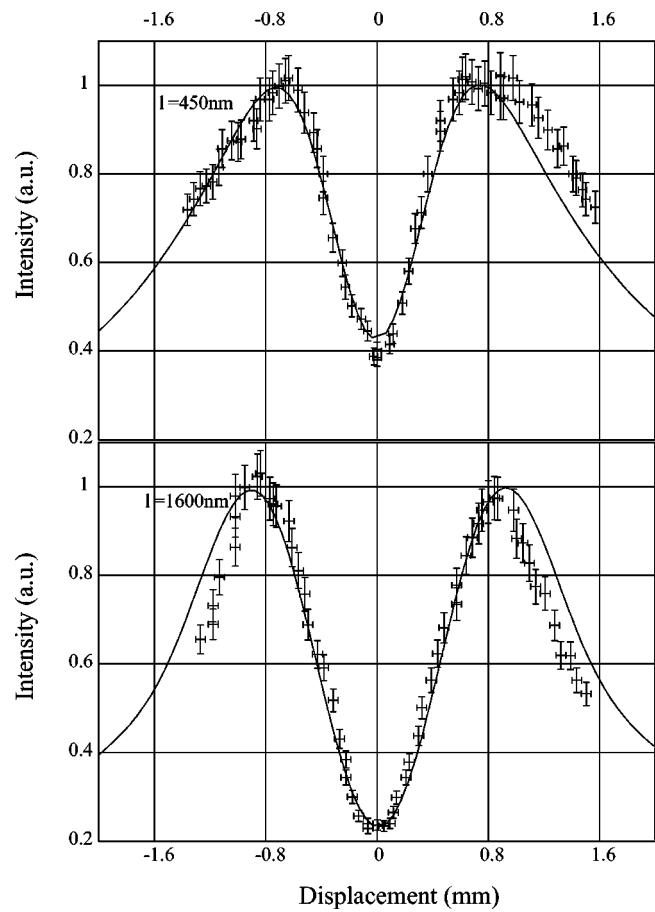


FIG. 5. $50 \mu\text{m}$ step scans of the central part in the vertical polarization case. Background level and normalization coefficients are the same as in the full-range scan (Fig. 4).

We thank R. Sorchetti, L. Cacciotti, and G. Fuga for their technical support, IESS group for realization of the silicon target, and the ELETTRA operation team for many hours of assistance in running the experiment.

- [1] N.F. Shul'ga and S.N. Dobrovolskii, *Pis'ma Zh. Eksp. Teor. Fiz.* **65**, 581 (1997) [*JETP Lett.* **65**, 611 (1997)].
- [2] N.F. Shul'ga, S.N. Dobrovolskii, and V.G. Syshchenko, *Nucl. Instrum. Methods Phys. Res. B* **145**, 180 (1998).
- [3] M. Castellano, V.A. Verzilov, L. Catani, A. Cianchi, G. Orlandi, and M. Geitz, *Phys. Rev. E* **63**, 056501 (2001).
- [4] V.A. Verzilov, *Phys. Lett. A* **273**, 135 (2000).

- [5] V.A. Verzilov, Laboratori Nazionali di Frascati, Report No. LNF-01/013(P), 2001 (unpublished).
- [6] B.M. Bolotovskii and G.V. Voskresenskii, *Usp. Fiz. Nauk* **88**, 209 (1966) [*Sov. Phys. Usp.* **9**, 73 (1966)].
- [7] R.A. Bosch and O.V. Chubar, in *Synchrotron Radiation Instrumentation*, edited by Ernest Fontes, AIP Conf. Proc. No. 417 (AIP, New York, 1997), p. 35.